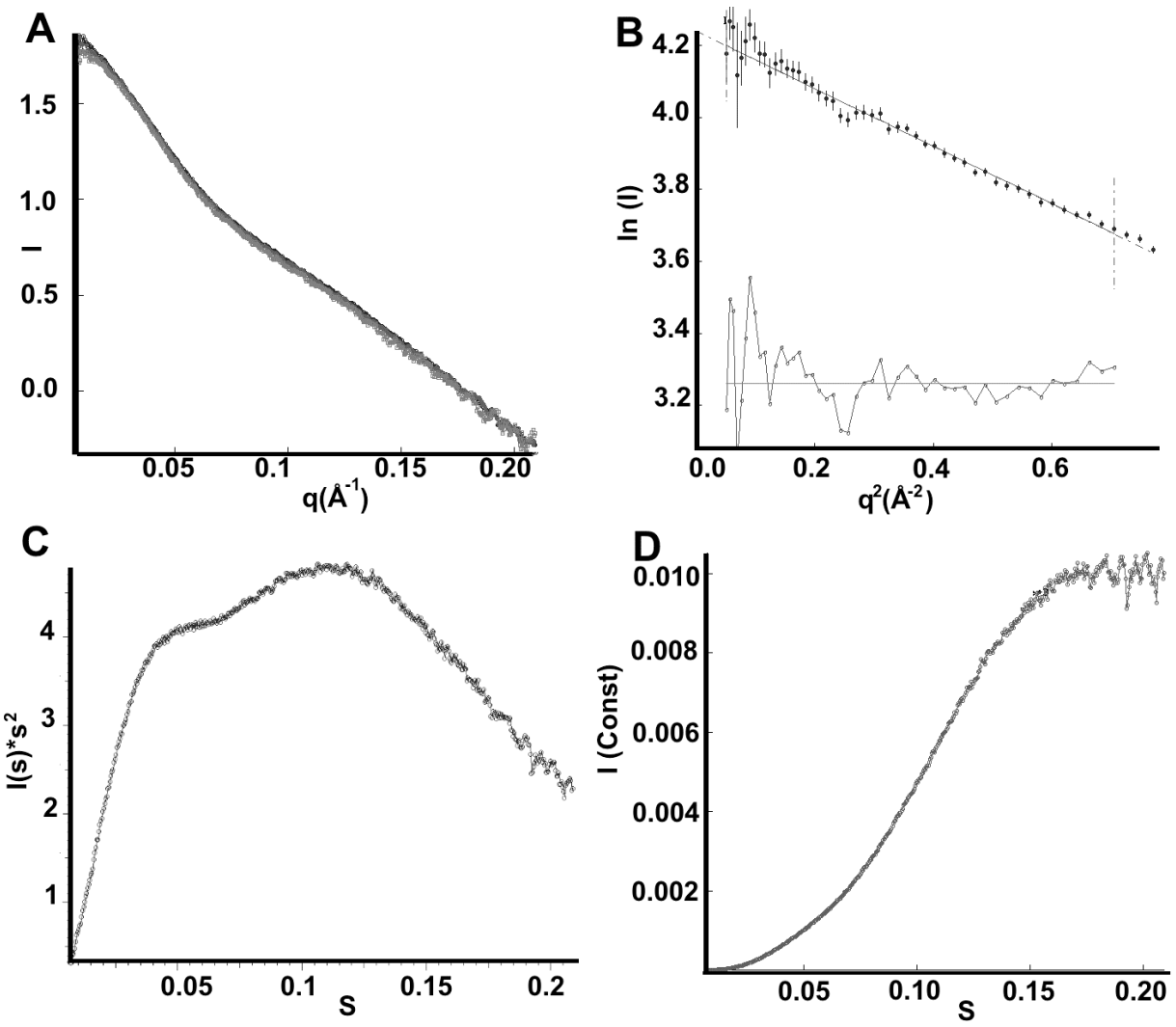

Supplementary Figure 1. parp486 SAXS raw data represented by Guinier, Porod and Kratky analysis. A) Superposition of raw parp486 SAXS data at 3, 6 and 9 mg/ml concentrations depicts minimal concentration dependent scattering effects. **B)** Guinier analysis of the low scattering angles depicts minimal aggregation. The residuals are illustrated in the lower portion of the graph. **C)** Kratky analysis of the data illustrates a folded, yet flexible particle. **D)** Porod graph of parp486 SAXS data determined that the sample follows Porod's law and has a volume of ~100,000Å^3.

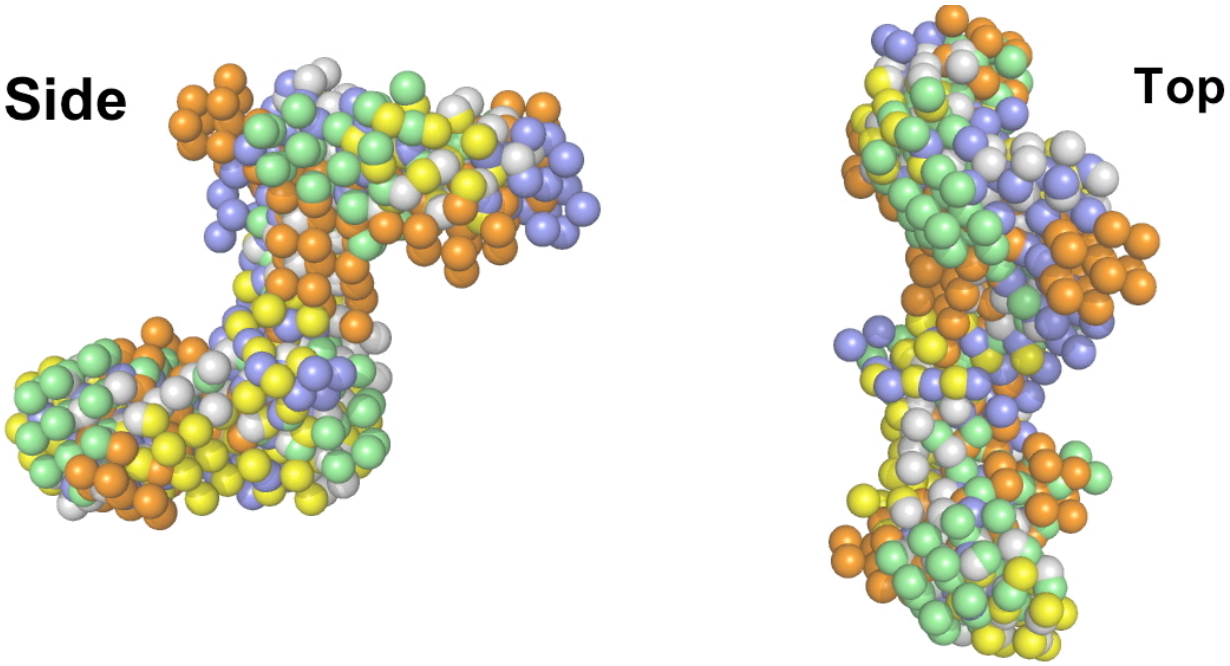

Supplementary Figure 2. Superposition of *ab initio* SAXS models of hparp486. The side (left) and top (right) views of five of the thirty averaged models that were used to create the final hparp486 particle reconstruction are shown. Each model is represented in a unique color. While the models do differ in certain areas, the overall shape of the particle remains similar. These models fit the SAXS scattering profile with a final χ^2 between 1.05-1.15.

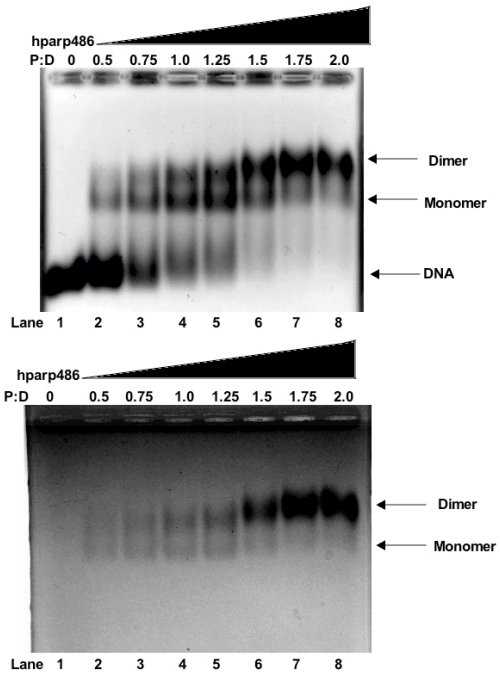

Supplementary Figure 3: EMSA of hparp486 interacting with a 53 base pair blunt ended DNA. Top: EtBr stain; bottom: Coomassie stain. The longer DNA fragment allows hparp486 to interact with DNA in either monomer or dimer form at hparp486:DNA ratios between 0.5-1.75. As the ratio of hparp486 increases, the dimer form becomes more prevalent. The longer DNA differs from the shorter fragments in which only monomeric interactions are detected both by EMSA and in solution using several different assays.

Supplementary Figure 4. Superposition of the SEC-MALS elution profiles of solutions containing either 2:1 molar ratios of hparp486-DNA complexes (peak 1), free hparp486 (peak 2) or free DNA (peak 3). In all cases peak 1 contains a 1:1 mixture of hparp486-DNA as well as free hparp486. This is noted by the decreasing molecular weight in the peak's shallow decent at increased volumes, as well as the significant overlap of the peak 1 with peak 2. The weight average molecular mass is superposed on each peak.

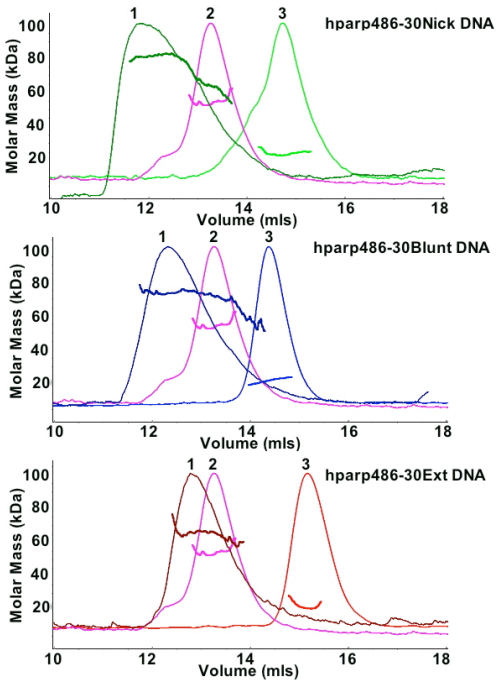

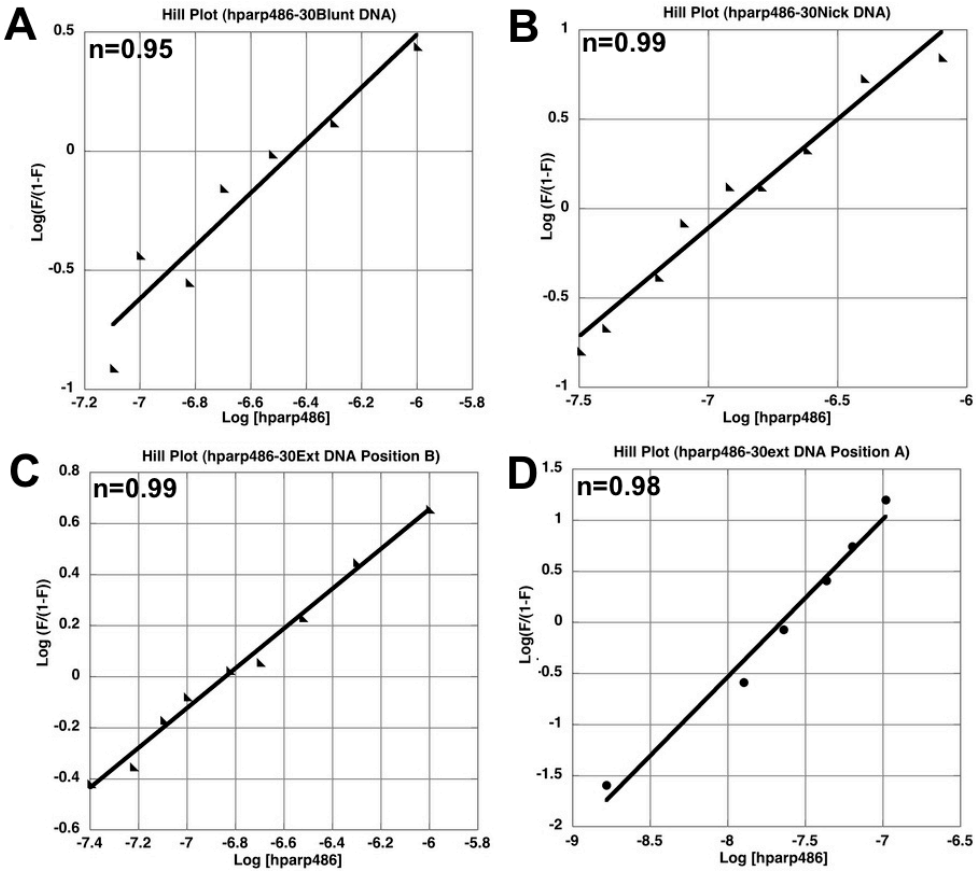

Supplementary Figure 5. Hill plots derived from the interactions of hparp486 with 30blunt, 30nick and 30ext DNA (A, B and C-D, respectively). In all cases, the slope of the line is less than 1(Table 3). The Hill coefficient is displayed in the upper left hand corner of each plot. Because the Hill coefficient is less than 1.0, these data reflect the lack of positive cooperativity in hparp486 interacting with each DNA damage model.

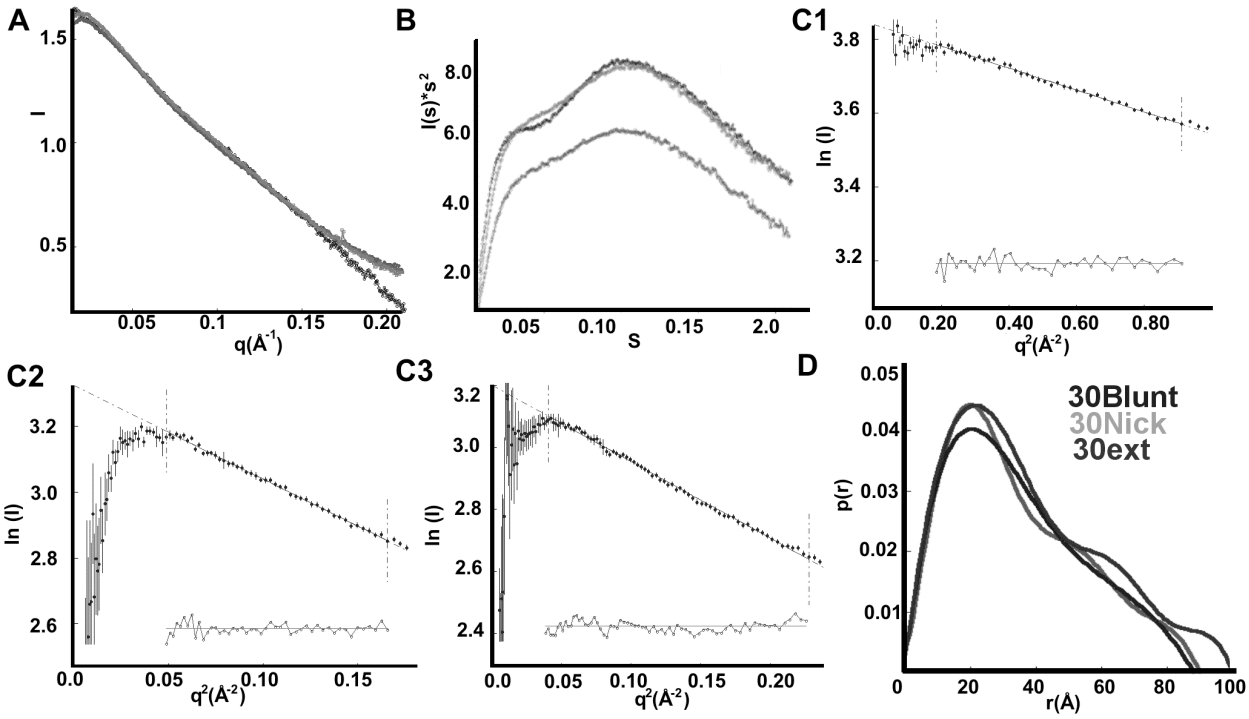

Supplementary Figure 6. Analysis of 30Blunt, 30nick and 30ext DNA SAXS data by Kratky, Guinier and P(r). A) Superposition of raw SAXS data for 30blunt, 30nick an 30ext DNA. **B)** Superposition of Kratky plots for each DNA illustrate that the 30nick and 30ext DNA do have some long range interactions. **C1-C3)** Guinier analysis similarly depict intermolecular interactions within the 30nick (C2) and 30ext' (C3) DNA samples. Blunt ended DNA (C1) remains homogeneous. The residuals are illustrated in the lower portion of each graph **D)** Superposed distance distribution functions of all DNAs. The data had 2-5 initial points truncated to remove the poor scattering at low angles. The resulting P(r) function portrays that all DNAs are between 88-100Å in the maximum dimension. This result is in agreement with either A or B double helical models.

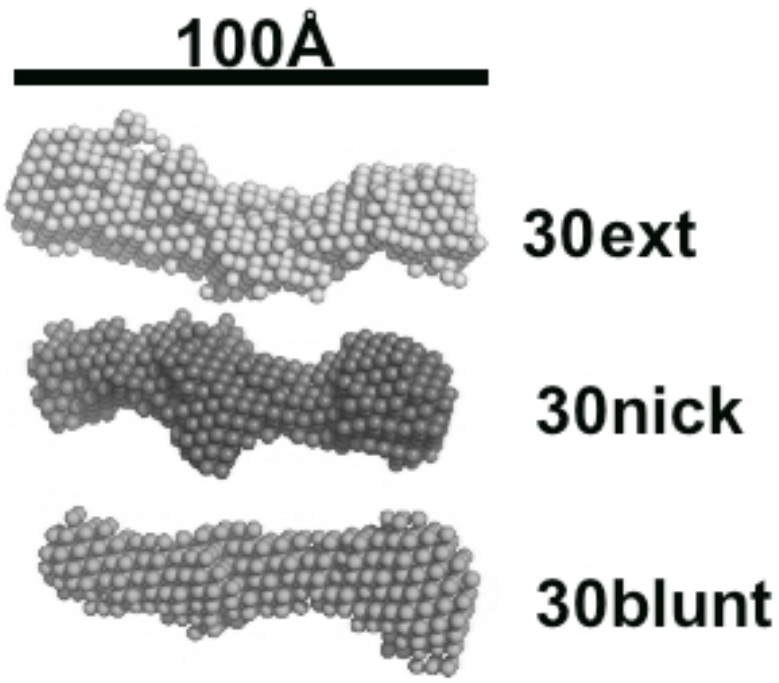

Supplementary Figure 7. ***Ab initio*** **models of 30ext, 30nick and 30blunt DNA samples.** The models were calculated from the average of ten DAMMIN *ab initio* models. The DNA models are all between 88-100Å in length, and cannot be differentiated from either B or A form DNA given the resolution of the technique.

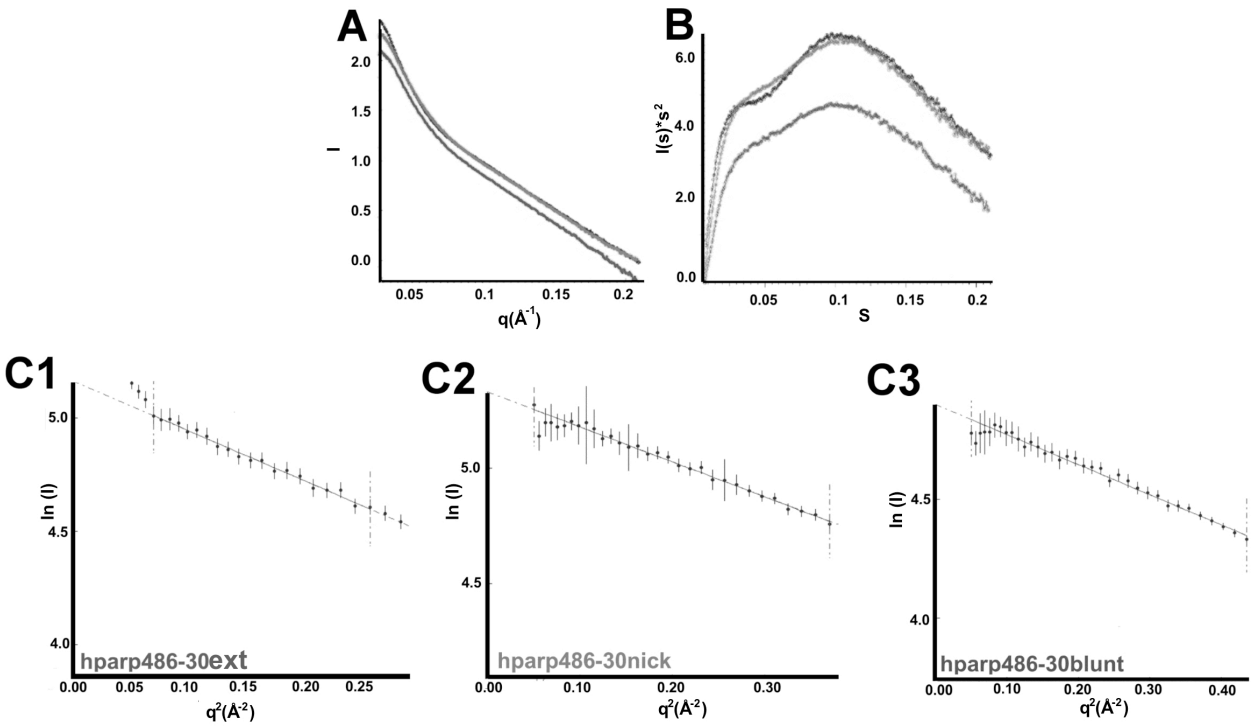

Supplementary Figure 8. Analysis of SAXS data for parp486 in complex with blunt, nicked and 6n3' DNA. A) Raw SAXS scattering for each protein-DNA complex. **B)** Kratky analysis of the complexes reveals an overall similar profile. **C1-C3)** Guinier analysis of each complex reveals that the data are devoid of aggregation.

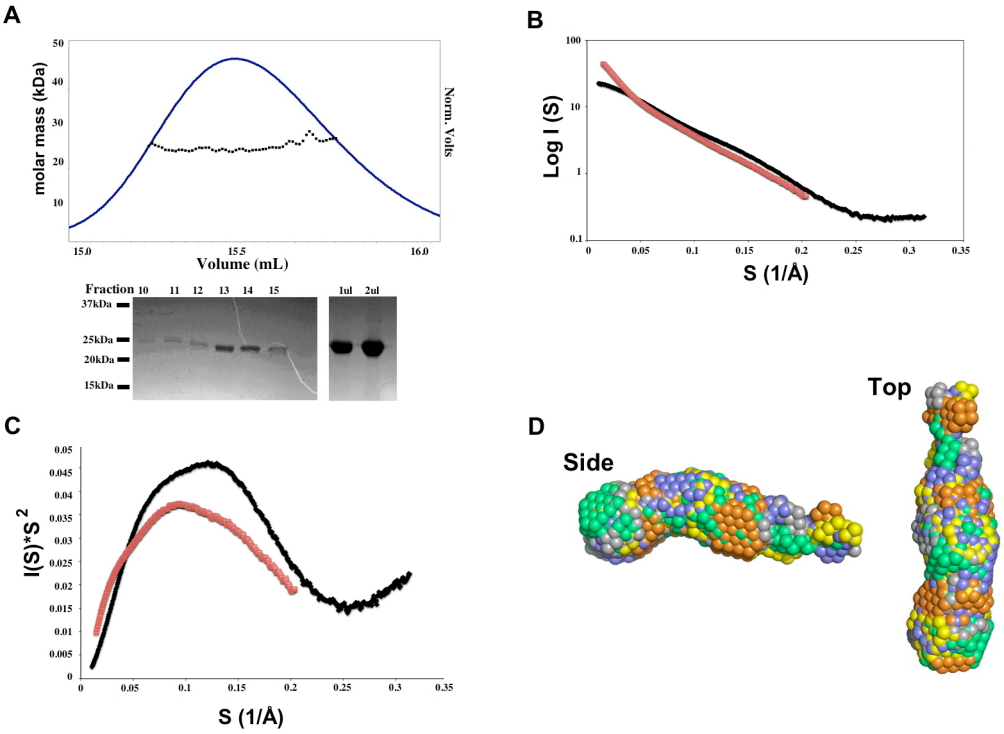

Supplementary Figure 9. Analysis of Purified hparp209. A) Top: SECMALS elution profile of purified hparp209 illustrates that the protein is a homogeneous monomer of with a molar mass of 22.5 kDa. **Bottom:** SDS-PAGE analysis of hparp209 from fractions of the SEC-MALS column reveal a singleband at approximately 23 kDa. 1 and 2 µl of the final concentrated protein fractions that were used for SAXS analysis are shown in the bottom right of panel A. **B)** SAXS scattering profiles of hparp209 (black) and the hparp209-30Blunt complex. **C)** Kratky analysis of hparp209 (black) and hparp209-30Blunt (red) complexes reveals that in both cases the particles have an overall ordered profile, albeit with some disorder at the higher scattering angles in the case of hparp209. **D)** Superposition of five ab initio particle reconstructions of hparp209 that fit the P(r) function (Fig. 5) with a chi square of 1.1 or better. The reconstructions reveal an over static shape with a small amount of terminal flexibility.